NASA-CR-203939

Final Report on

NASA SCAR

Contract #NASW-4515

Technical Period of Performance: 10/90 to 6/94

Prepared by:

Robert J. Lang

Senior Research Section Manager, SDL, Inc.

80 Rose Orchard Way, San Jose, CA 95134

Tel: 408-943-9411 Fax: 408-943-1070

TABLE OF CONTENTS

1.0. INTRODUCTION

1.1. Executive Summary

This report describes work performed by SDL in the development of monolithically-integrated master oscillator power amplifiers under the NASA-SCAR research contract. Technical performance on the contract extended over three years and eight months, divided into a base period (Phase I) and two options (Phases II and III). The goals of the program were to demonstrate high power diffraction-limited operation from a semiconductor laser with the following characteristics:

1) Output power of 0.5 to 1.0 W continuous-wave (cw)

2) Single spectral mode with greater than 20 dB of side mode suppression

3) Single spatial mode operation

4) Modulation capability of 0.5 GHz

5) Operating wavelength between 830-860 nm

All of the goals of this contract were either met or exceeded. cw diffraction-limited output powers as high as 2.2 W were achieved while maintaining a single longitudinal mode. Side mode suppression ratios greater than 20 dB are typically obtained. The single spatial mode output has a Strehl ratio estimated at 0.85, and a high-speed modulation capability was demonstrated with a small-signal 3-dB roll-off at 1.0 GHz. Finally, all of this performance was obtained in the 860 nm wavelength band, which corresponds to the peak sensitivity of Si detectors. During the first option period, three deliverables were fabricated and delivered that included 1 distributed Bragg reflector (DBR) laser operating at 970 nm, 1 DBR laser operating at 860 nm, and one monolithic flared amplifier master oscillator power amplifier (MFA-MOPA) providing 0.5 W cw diffraction-limited output. During the second option period, a total of 5 MFA-MOPA devices were delivered, each operating to better than 1 W cw diffraction-limited at 860 nm.

1.2. Technical Approach

The objective of the SCAR program was to develop a diode laser source suitable for satellite optical cross links, i.e., with high diffraction-limited output power and high-speed modulation capability. At the onset of this program (October, 1990) the highest diffraction-limited output powers from diode lasers were obtained from single-stripe Fabry-Perot (cleaved facet) structures. Although the performance of Fabry-Perot diode lasers (indicated by black circles in figure 1.1) improved steadily through the 1970s and 1980s, their performance began to level off during the late 1980s in the 150–200 mW range. The demands of optical satellite communication links,

however, are in the 500 mW and up range, necessitating an advanced diode laser development effort with aggressive power and spectral beam quality goals.

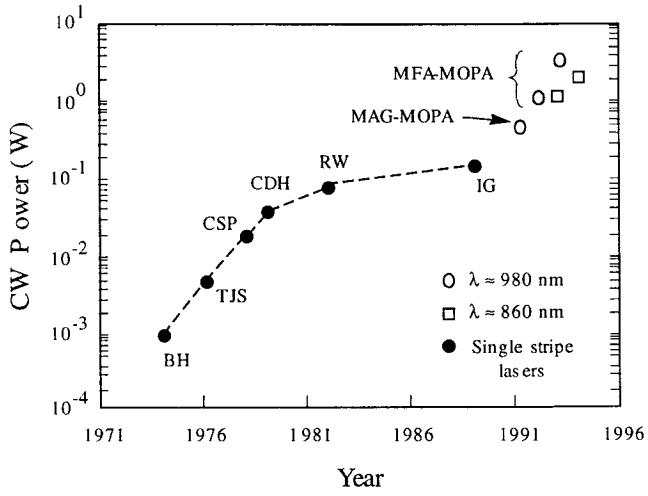

Figure 1.1. Single spatial mode power from conventional single stripe and MOPA semiconductor laser versus time

Although the speed and spectral requirements are significant, the primary technical challenge in meeting the goals of the SCAR program has been to obtain a high cw diffraction-limited output power. In the course of the SCAR program, two approaches to achieve high diffraction-limited powers have been investigated. Initially, a monolithic active grating master oscillator power amplifier (MAG-MOPA) architecture at 860 nm was investigated, based on promising results obtained from strained-layer InGaAs MAG-MOPA lasers at 980 nm. However, approximately halfway through the program, encouraging developments in strained-layer flared amplifiers spurred a redirection of the SCAR program to a monolithically integrated flared amplifier master oscillator power amplifier (MFA-MOPA) architecture. This redirection resulted in a rapid and dramatic improvement in the device performance, to the extent that the highest power 860 nm MFA-MOPA demonstrated (2.2 W cw diffraction-limited) is over 10× higher than the rated output of the best commercially available single-stripe lasers. This leap to the greater than 1 W cw power level has dramatic implications for long distance high speed free-space laser communication systems.

Over the course of the contract, several technologies have been developed that led to the successful realization of a >1 W cw diffraction-limited source. Section 2 presents a detailed discussion of the development of high power distributed Bragg reflector (DBR) lasers for master oscillators at 860 nm. Section 3 discusses the integration of the 860 nm DBR laser into a MAG-MOPA architecture. Section 4 introduces the MFA-MOPA architecture and details the development of high

performance 860 nm MFA-MOPAs. Sections 5 and 6 present a summary and a list of references, respectively.

2.0. DISTRIBUTED BRAGG REFLECTOR LASERS

All MOPA architectures, including both the MAG-MOPA and MFA-MOPA, require a high quality single spatial mode master oscillator. The master oscillator determines the spectral properties of the MOPA such as the side mode suppression ratio and the linewidth; in addition, the spatial beam quality is also strongly affected by the beam quality of the master oscillator. For maximum efficiency, the master oscillator must also provide high single spatial mode power to fully saturate the gain of the amplifier. Most importantly, in a monolithic MOPA architecture, the master oscillator is monolithically integrated with the power amplifier and cannot rely on cleaved facets for feedback. A narrow-stripe distributed Bragg reflector laser addresses all of the requirements placed on a master oscillator; it can be single-spatial-mode and single-longitudinal-mode, can provide output powers of ~100 mW, and is intrinsically integrable with other photonic components. Therefore, the SCAR research program initially focused on the development of high power, single-frequency DBR lasers using a reliable buried grating process.

A distributed Bragg reflector laser was designed and fabricated using a two-step metal-organic chemical vapor deposition (MOCVD) process. A schematic diagram of the DBR structure is shown in Figure 2.1. The optical waveguide is a standard AlGaAs separate-confinement heterostructure with an GaAs quantum well centered in the active region. The initial epitaxial growth is stopped just after a portion of the p-side AlGaAs cladding layer is grown and the wafer is removed from the reactor. Second-order gratings are patterned using photolithographic and holographic exposure to define high and low reflectivity mirrors surrounding a 500 μm gain region. After grating formation, p-type cladding and capping layers are regrown by MOCVD. The grating teeth are approximately 80 nm high yielding an estimated modal overlap with the gratings of 12% and an estimated modal overlap with the GaAs quantum well of 2%.

The real refractive index waveguides formed are 3–4 μm wide and extend through both the gain and grating regions. Standard metallization and implant techniques are used to define the 500 μm gain regions. Discrete DBR lasers are formed by cleaving front and back grating lengths of 150 and 500 μm, respectively. Anti-reflection (AR) coatings with reflectivities on the order of 1-2% are deposited on each of the two cleaved facets. For cw operation devices are mounted p-side down on heat sinks.

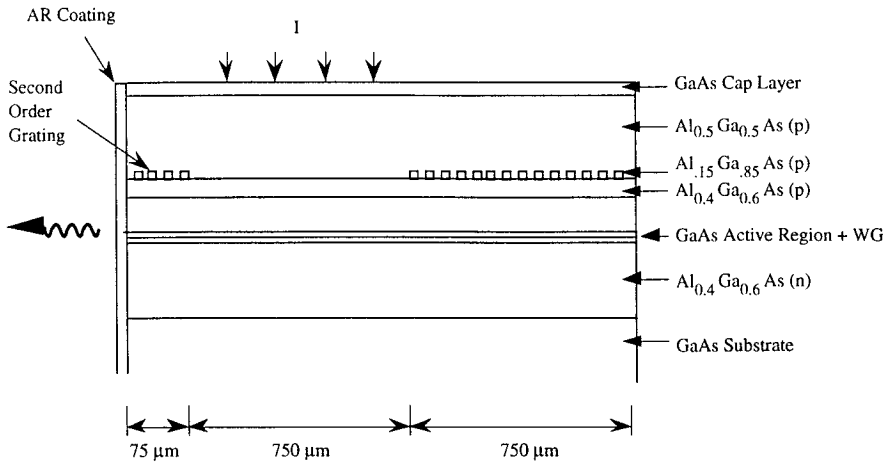

Figure 2.1. Schematic of an 860 nm DBR laser structure.

Optimization of the performance of a DBR laser requires careful control over the grating reflectivity. Although the grating reflectivity can be calculated from the mode profiles of the epitaxial structure, the thickness of the grating layer, and the duty cycle of the grating, it is necessary to experimentally verify the strength of the coupling coefficient and grating reflectivity. This measurement can be carried out by comparing the threshold current of a DBR laser with one grating mirror to the threshold current of uncoated Fabry-Perot lasers. The threshold current density in A/cm^2 is linear with cavity loss in the relation

$$J_{th} = J_0 + const \cdot \frac{1}{L} \ln \frac{1}{R_1 R_2}, \tag{2.1}$$

where J_{th} is the threshold current, J_0 is the transparency current density, L is the length of the laser and R_1 and R_2 are the mirror reflectivities. By measuring the threshold current for several uncoated cleaved devices (R_1 =R_2 =0.29), the slope of equation (1) may be determined; from this relation and the threshold current of the DBR laser, the mirror reflectivity may be calculated. This relationship is shown in figure 2.2.

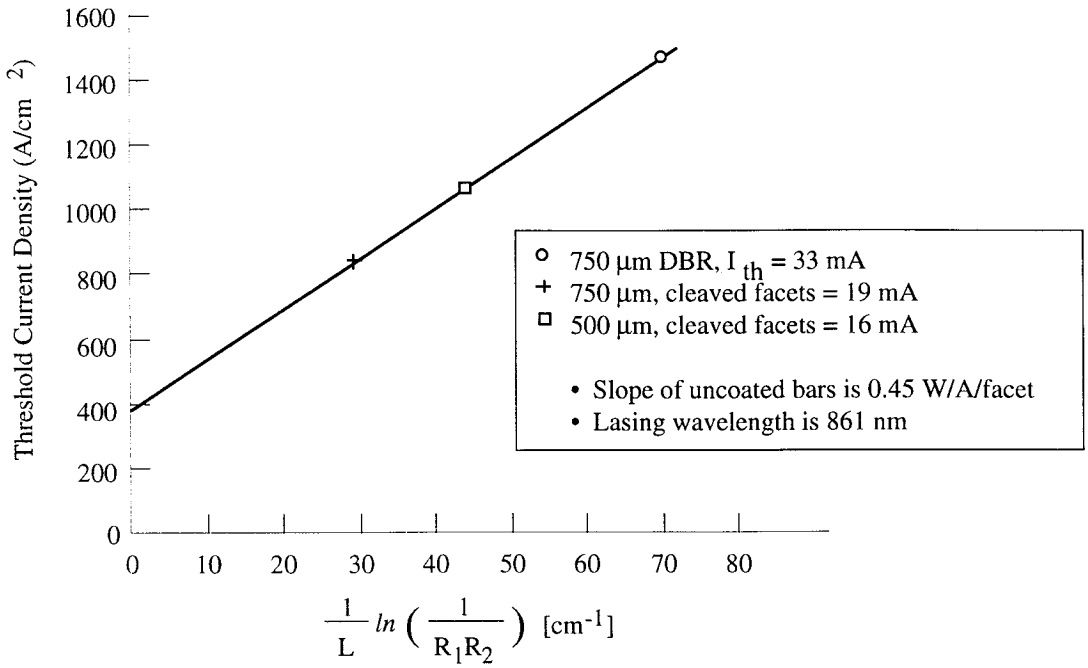

Figure 2.2. Threshold current of Fabry-Perot and DBR lasers.

From this relationship we can infer a grating reflectivity of 36%.

The light-current curve for the 860 nm DBR laser is shown in figure 2.3. The output power is as high as 80 mW cw at room temperature. The spectrum at 50 mW is shown as an inset to the figure. The device operates in a single longitudinal mode over the entire power range.

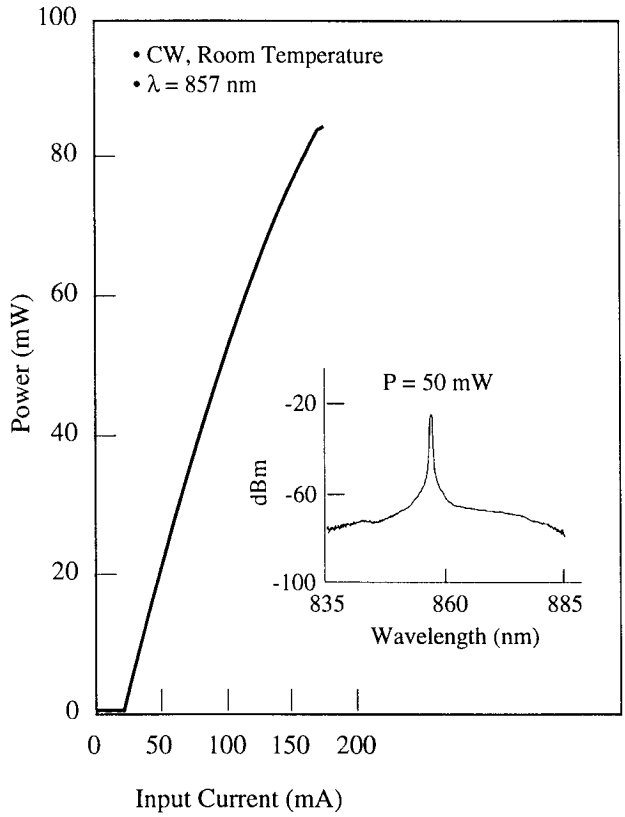

Figure 2.3. Light-current curve and spectrum of an 860 nm DBR laser.

Far fields for the 860 nm DBR laser are shown in figures 2.4(a) and (b). The lateral far field is single-lobed with a full width at half maximum of 11.7° and does not broaden or steer with increasing power. The far field perpendicular to the junction is 29.7°, corresponding to the ~1 μm waveguide thickness of the epitaxial structure.

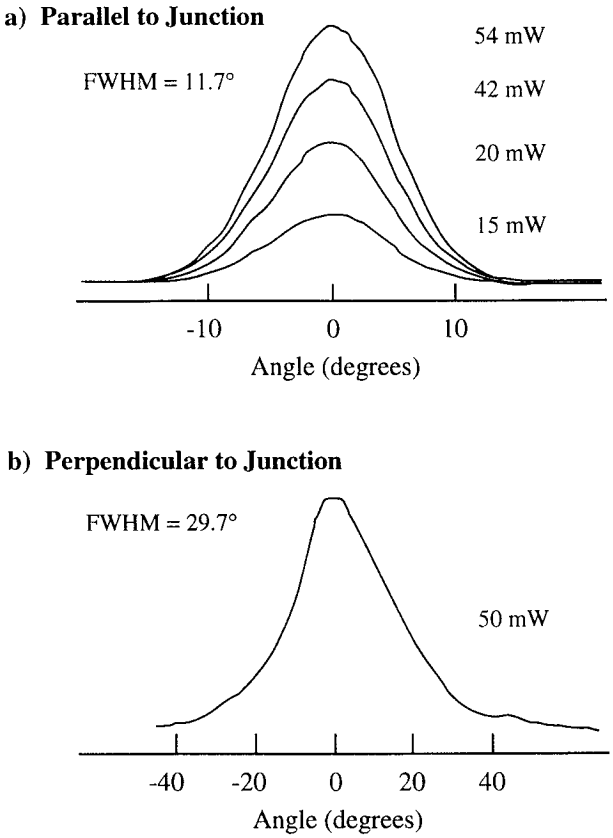

Figure 2.4. Far fields of an 860 nm DBR laser. (a) parallel to the junction, (b) perpendicular to the junction.

DBR lasers are intrinsically single-longitudinal mode and can be tuned by either current or temperature. The thermal tuning characteristic of the 857 nm DBR laser is shown in figure 2.5. The tuning is linear and continuous over a greater than 30° temperature variation with a slope of 0.5Å/K. Thermal tuning comes from the change in effective refractive index with temperature, and is typically 0.5–0.7 Å/K in GaAs-based lasers.

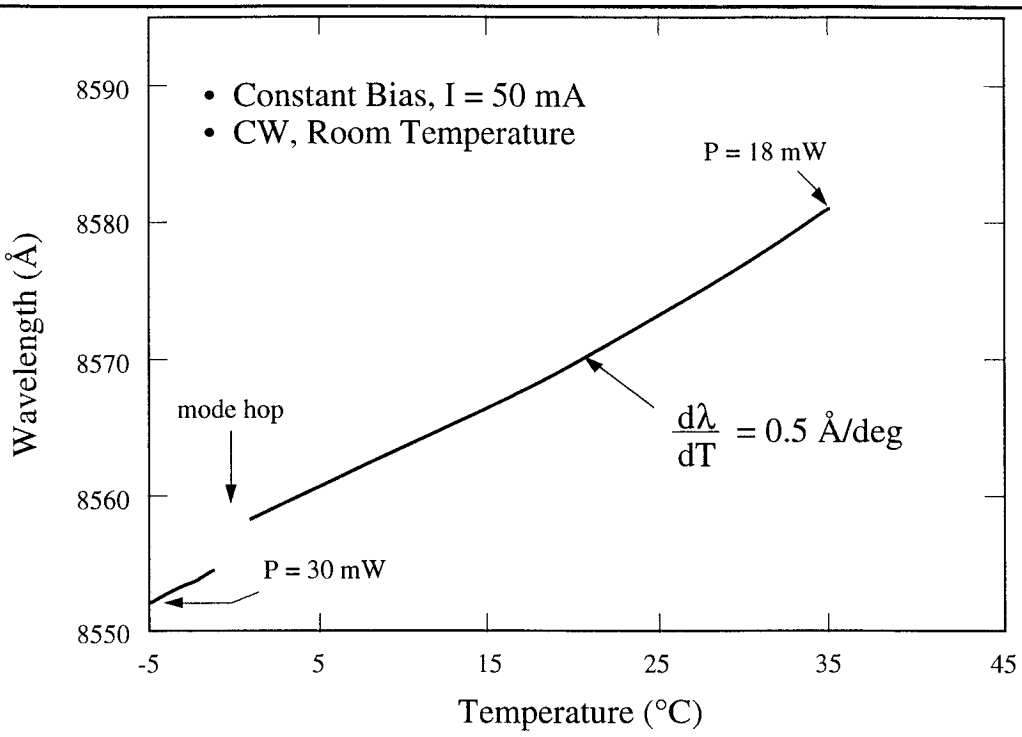

Figure 2.5. Thermal tuning of an 860 nm DBR laser.

There is also some tuning with injection current, due to inhomogeneous heating of the laser structure that alters the phase relationship between the front and back mirrors. Current tuning of DBR lasers typically includes a number of mode hops, but has the advantage of faster tuning than is possible with temperature tuning of the entire diode. The current tuning characteristic is shown in figure 2.6.

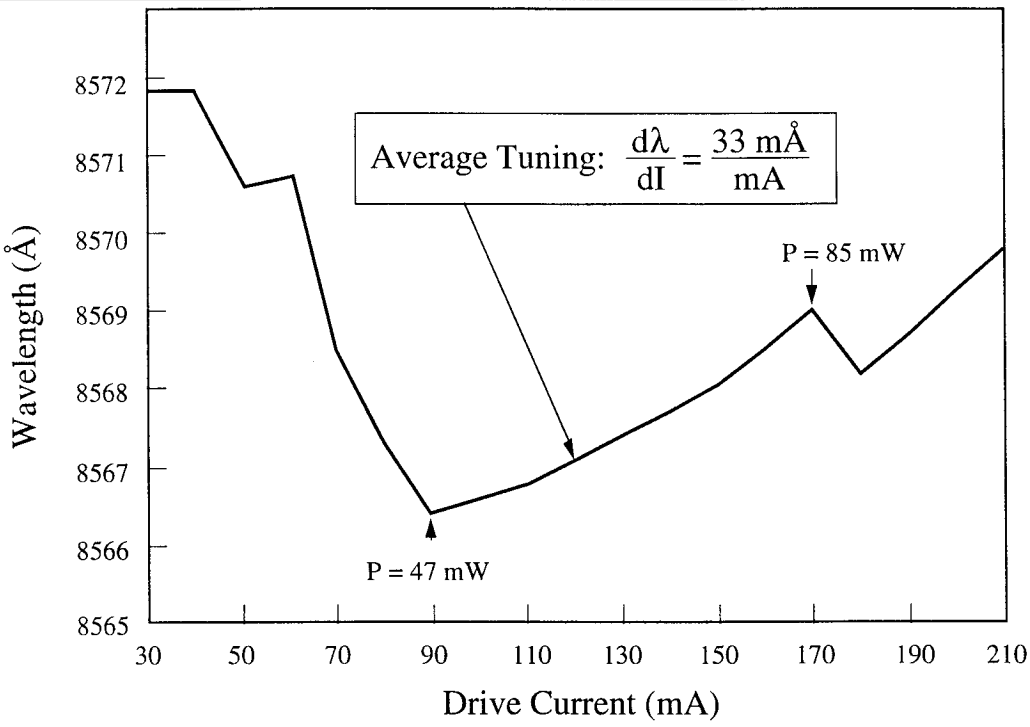

Figure 2.6. Current tuning of an 860 nm DBR laser.

This level of single-mode performance is comparable to that obtained from conventional Fabry-Perot lasers with the addition of monolithic integrability and single-longitudinal-mode operation. The DBR lasers were thus suitable for integration with a power amplifier to further increase the diffraction-limited output power.

3.0. MONOLITHIC ACTIVE GRATING MOPAS

The initial approach undertaken in the SCAR program to achieve a high diffraction-limited output power was the monolithic active grating master oscillator power amplifier (MAG-MOPA). A schematic diagram of a MAG-MOPA is shown in Figure 3.1. The MAG-MOPA consists of a single mode DBR master oscillator monolithically integrated with a preamplifier and an active grating power amplifier. The active grating power amplifier consists of a long single mode waveguide containing a detuned grating, i.e., a grating that has no in-plane diffraction order. The first order diffraction component from the grating is deflected out of the plane of the device, slightly forward of normal, as shown in figure 3.1.

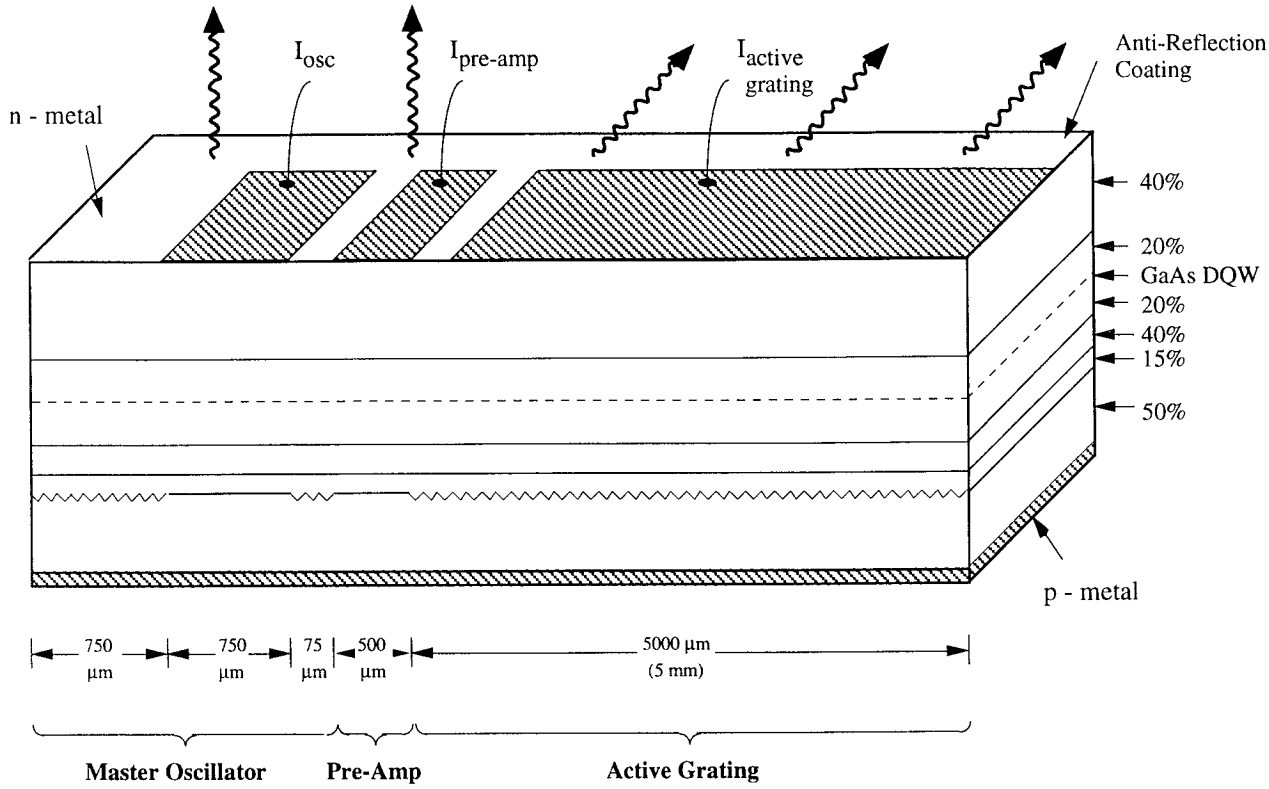

Figure 3.1. Schematic of a MAG-MOPA.

The active grating amplifier is electrically pumped and continuously diffracts light out of the single-mode waveguide; at the same time that the field is depleted by the grating output coupler, it is restored by the optical gain provided by the electrical pumping. Within a few hundred microns, a balance between optical gain and grating output coupling loss is obtained and the guided wave intensity saturates to a fixed steady-state value, at which point the saturated local gain equals the guided-mode losses. The guided mode loss consists of scattered radiation loss (α_s), which is the desired output coupling, and distributed optical losses (α) of a few cm^{-1}. Once this equilibrium is reached, the guided-wave power and the local carrier density remain constant along the remaining length of the active grating aperture as the gain from the injected current equals the losses.

As a result of the constant carrier density, the phase of the radiated wavefront is flat along the length of the amplifier and the output is diffraction-limited in the longitudinal direction. Because the beam is emitted from a single-mode waveguide, it is also diffraction-limited in the lateral direction, and the resulting output is a cylindrical wavefront with a virtual source approximately 3×4000 µm. Previous MAG-MOPA devices have been demonstrated to produce diffraction-limited, single-lobed output powers in excess of 800 mW pulsed and 530 mW cw at 980 nm, making the MAG-MOPA structure a strong candidate for high power diffraction-limited operation at 860 nm.

The epitaxial structure for an 860 nm MAG-MOPA is shown in figure 3.2. It has a GaAs quantum well active layer with surround layers of AlGaAs to insure their transparency. The layers are grown on a GaAs substrate, which is extremely absorptive at 860 nm. For junction-down devices, additional steps must be taken to avoid absorption of the output beam in the substrate.

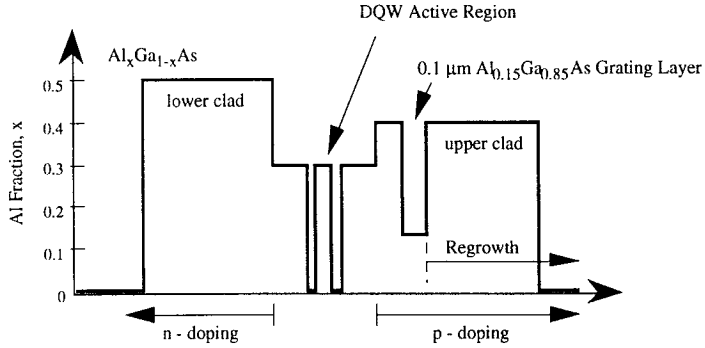

Figure 3.2. Epitaxial structure of the 860 nm MAG-MOPA.

To address the issue of substrate absorption, three geometries were initially investigated. The first is shown in figure 3.3. In this configuration, the MAG-MOPA is mounted p-up and the emission is coupled out through the top surface. A set of superlattice reflectors is implemented beneath the waveguide to reflect the downward-coupled radiation back up to the surface. The p-side contact is made to a highly p-doped GaAs cap layer, which is removed over the waveguide; current is conducted laterally from the cap layer through the upper cladding layers and into the waveguide.

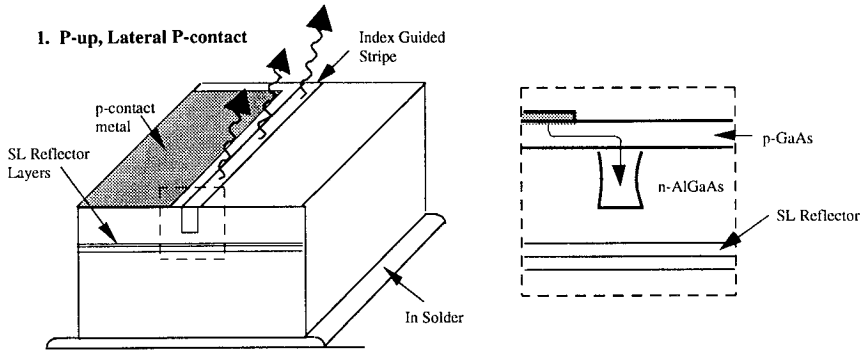

Figure 3.3. Schematic of a p-up 860 nm MAG-MOPA.

The advantage of this configuration is that it is easily implemented using standard bonding techniques. There is no need to remove the substrate. However, the placement of the superlattice reflector layers is critical for efficient performance, since efficient output coupling requires that the phase of the downward-going beam reflected off of the superlattice reflectors match the phase of the upward-going beam. In addition, the requirement of lateral conduction through the p-type GaAs leads to a high series resistance. Additionally, the thermal resistance of the device is

significantly higher than a p-down device, due to the relatively poor thermal conductivity of the GaAs substrate as compared to that of the submount.

The second investigated geometry is shown in figure 3.4. The device is mounted p-down, but the substrate is removed in a narrow trench over the active layer by wet etching. The current is conducted from the top contact through the substrate and then laterally through the upper layers of the trench. This architecture has the advantage that there is no superlattice reflector — the downward-going beam is reflected by the p-side metallization — and the thermal resistance of the device is low due to the p-side mounting.

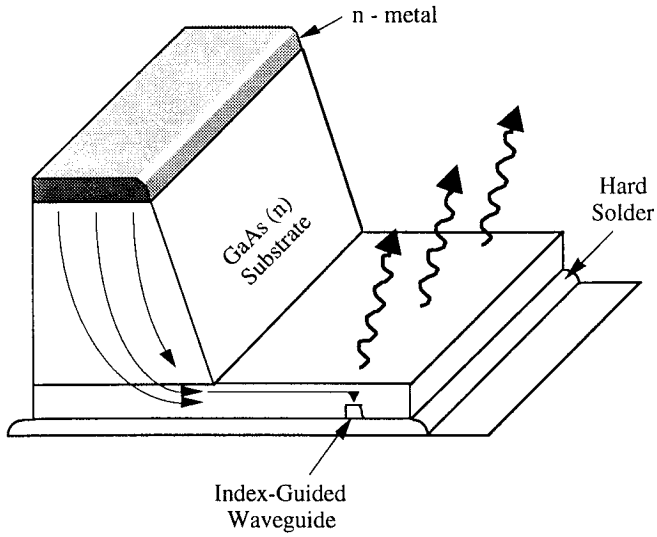

Figure 3.4. Schematic of a p-down mounted MAG-MOPA. Current is injected from a contact on the top (n-side) and is conducted laterally to the active layer.

However, this architecture, too, poses fabricational challenges. The regions with the substrate removed are only 3–4 μm thick and are thus extremely fragile during subsequent processing. More importantly, the relatively long current path through the Al-containing cladding layers gives a high series resistance to the device.

To reduce the series resistance, this structure was modified to extend the *n*-side contact down into the trench to contact the cladding layers of the waveguide directly, as shown in figure 3.5. By performing a metallization after the trench was etched, the n-side contact could be formed within a few μm of the active layer, reducing the current path length by over an order of magnitude and reducing the series resistance correspondingly.

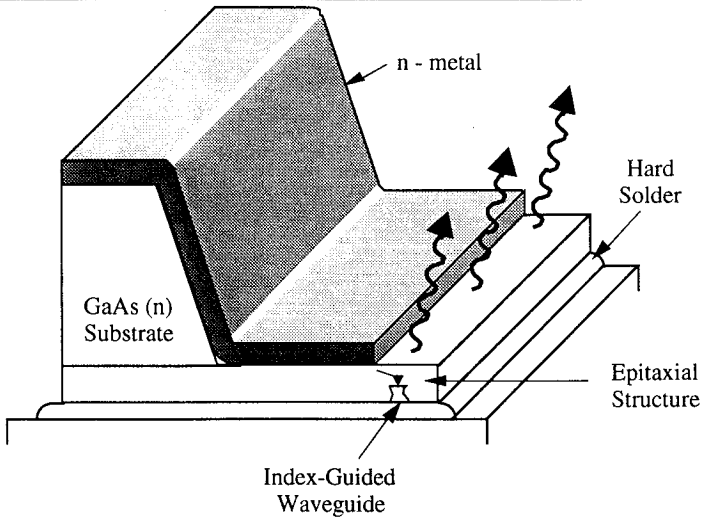

Figure 3.5. Schematic of the MAG-MOPA with metallized trench.

This configuration presents greater processing challenges, since several processing steps must be performed after the trench has been etched. However, the device performance is significantly enhanced. Figure 3.6 shows the bonding configuration for the MAG-MOPA. The oscillator, pre-amplifier, and active grating were separately contacted to permit individual characterization of the three elements of the MOPA.

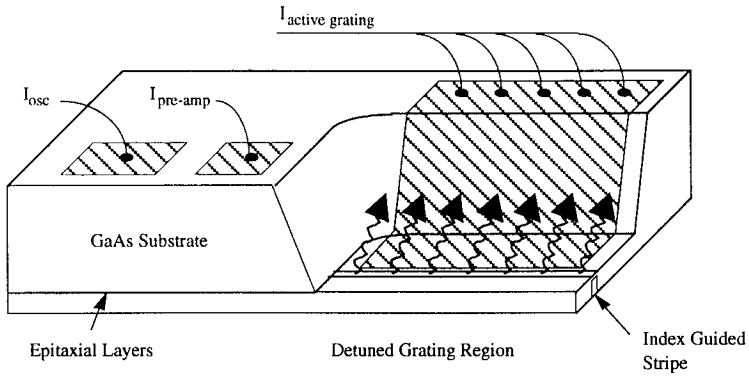

Figure 3.6. Schematic of the bonding configuration for the 860 nm MAG-MOPA.

Figure 3.7 shows a plot of the surface-coupled near field intensity above an 860 nm MAG-MOPA, which shows the light distribution within. (The reflective gratings of the DBR master oscillator are second-order gratings and therefore couple out light perpendicular to the surface.) The active grating in this measurement was unpumped. With the active grating unpumped, the coupling coefficient can be inferred from the $1/e$ decay length of the intensity within the active grating. The penetration depth is approximately 400 cm^{-1}, which yields a total decay factor α of 21

cm^{-1}. Combining this result with the intrinsic absorption/scattering loss of 5 cm^{-1} yields a grating coupling coefficient of κ=16 cm^{-1}.

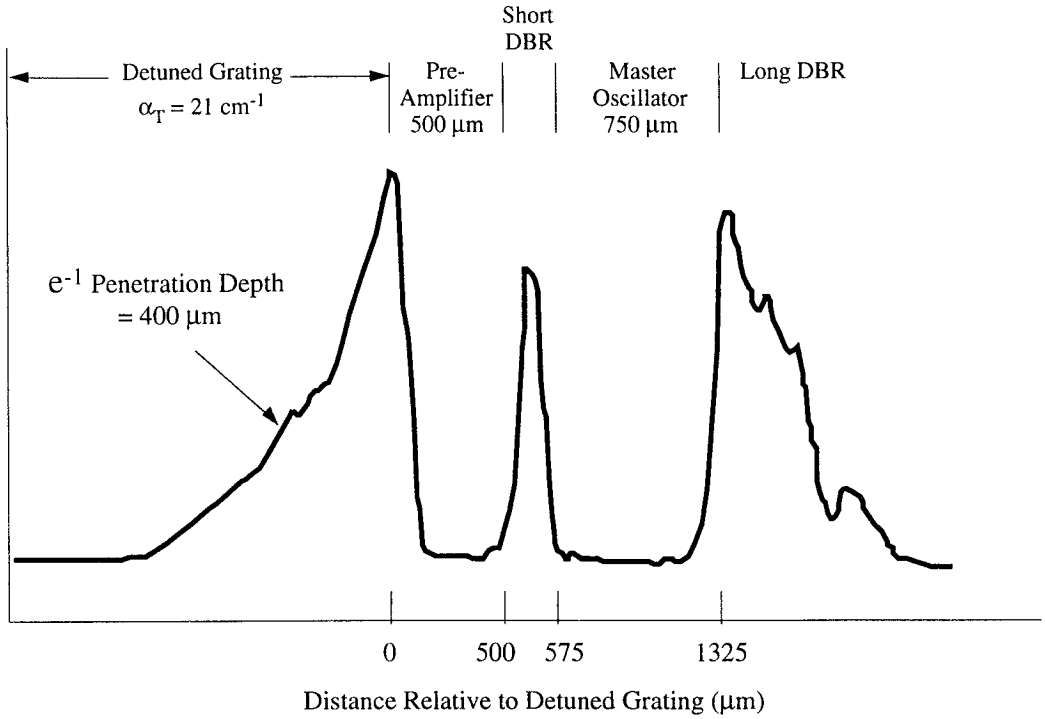

Figure 3.7. Surface-coupled near field intensity along the 860 nm MAG-MOPA.

Initial characterization of the MAG-MOPA was carried out with both the preamplifier and active grating unpumped. The surface-coupled output power versus master oscillator current is shown in figure 3.8. The oscillator threshold was approximately 40 mA. The slope efficiency is relatively low because a large fraction of the light is reflected at the (uncoated) top surface of the waveguide. Correcting for the effects of reflection gives a corrected slope of 0.35 W/A.

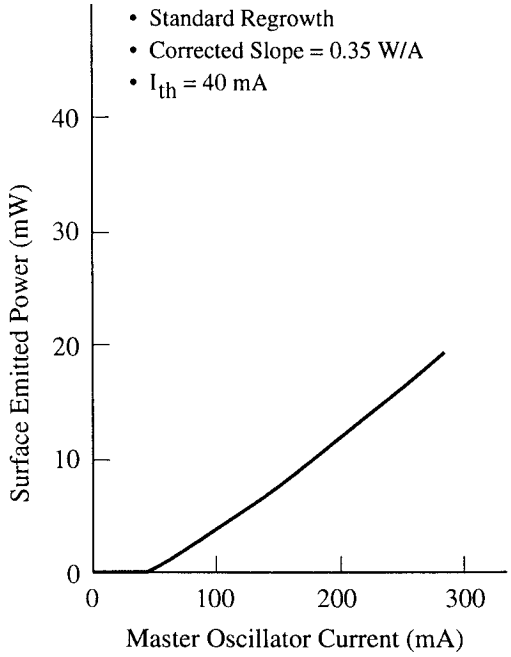

Figure 3.8. Light-current curve of 860 nm MAG-MOPA with active grating unpumped.

This efficiency is still a factor 2–3× below that of edge-emitting lasers. A new epitaxial structure was designed to maximize the overlap between the waveguide mode and the gain region. MAG-MOPAs were fabricated from this new structure and characterized, again, with the active grating unpumped.

The surface-emitted output power as a function of master oscillator current (with the pre-amplifier unpumped) is shown in figure 3.9. With the new epitaxial design, the threshold current was reduced by a factor of 2 to a value of 21 mA and the slope efficiency, corrected for the effects of top surface reflection, was raised to 0.7 W/A.

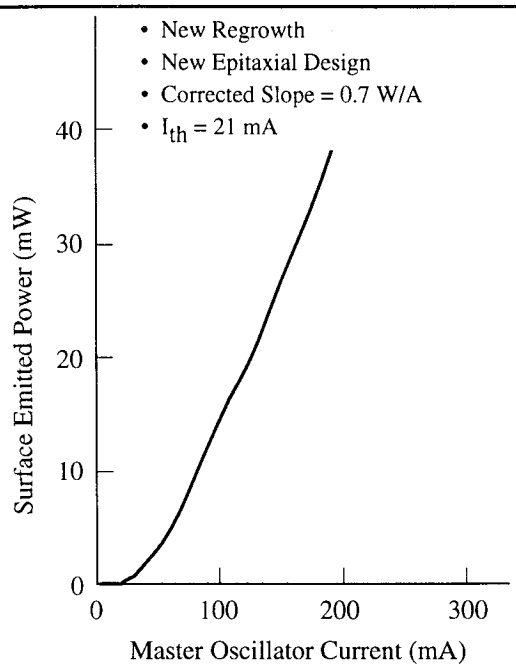

Figure 3.9. Surface-coupled light-current curve for the master oscillator with revised epitaxial structure.

The preceding data were taken with the preamplifier unpumped. By forward biasing the preamplifier, considerably higher output powers may be obtained. Figure 3.10 shows the output power as a function of preamplifier current for several fixed values of master oscillator current. The total slope efficiency (with respect to master oscillator current + preamplifier current) is 0.65 W/A (again, corrected for the effects of grating coupling efficiency and surface reflection). The corrected slope efficiency of the preamplifier alone is 0.78 W/A, comparable to efficiencies obtained in edge-emitting devices.

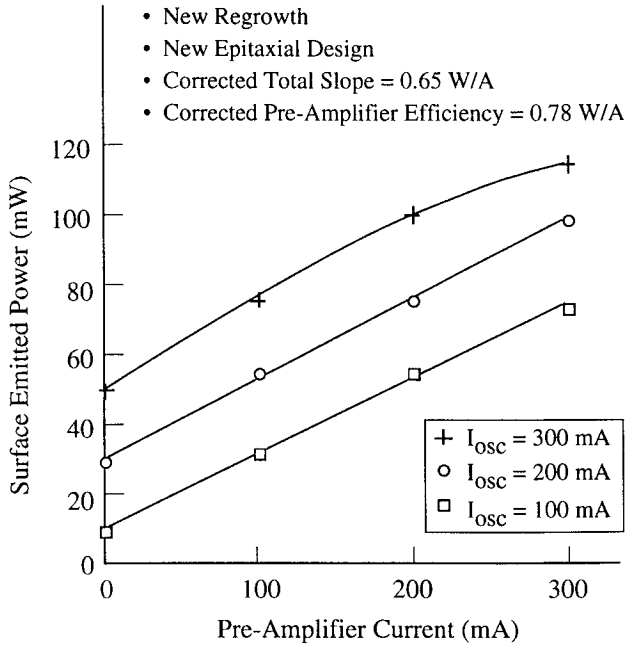

Figure 3.10. Surface-coupled output power versus preamplifier current for fixed oscillator current.

The preceding data were taken under pulsed conditions. Under cw operation, approximately 100 mW of output power was obtained in a surface-emitted diffraction-limited beam.

4.0. MONOLITHIC FLARED AMPLIFIER MOPAS

4.1. MFA-MOPA Background

During the first year of the SCAR program, a 980 nm discrete flared amplifier was demonstrated to provide diffraction-limited powers in the ~1 W range. Within a matter of months, SDL had demonstrated a new architecture based on flared amplifiers, the MFA-MOPA, which demonstrated in excess of 1 W cw diffraction-limited operation at 980 nm (i.e., with an InGaAs active layer). The MFA-MOPA architecture showed great promise for diffraction-limited sources and was incorporated into the design goals of the SCAR program.

The design of the 980 nm MFA-MOPA, presented in Figure 4.1, incorporates a single-mode distributed Bragg reflector (DBR) master oscillator monolithically coupled to a flared power amplifier. The output of the DBR master oscillator is injected into the flared amplifier where the spatial mode of the waveguide is allowed to freely diffract as it is amplified. Reliable high power operation is obtained by maintaining an approximately constant optical intensity in the output beam while power scaling is achieved by linearly expanding the aperture width.

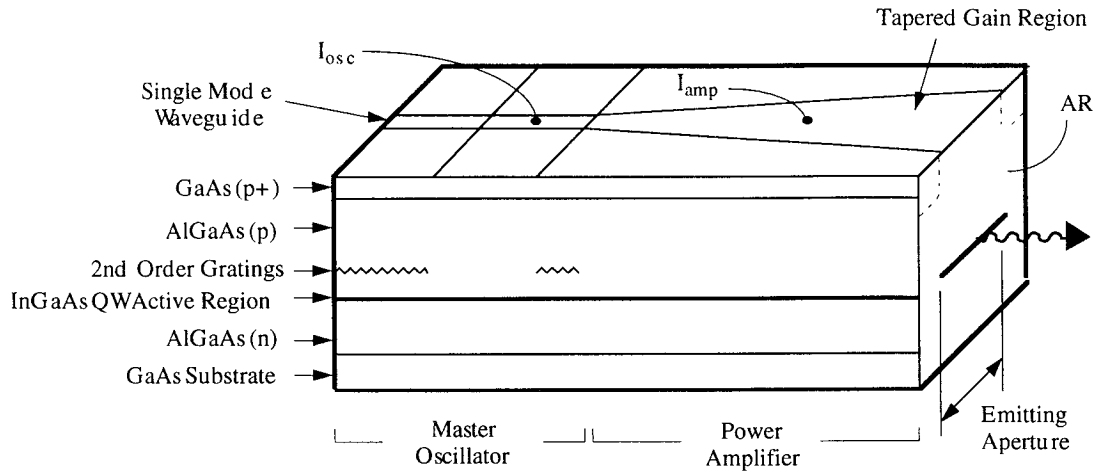

Figure 4.1. Schematic diagram of a 980 nm MFA-MOPA structure with an InGaAs QW active region.

Advantages of the MFA-MOPA design include:

(1) The single emitting aperture of the MFA-MOPA results in a single, diffraction-limited beam and can be collimated with simple spherical and cylindrical optics.

(2) The gain of the flared amplifier in the MFA-MOPA can be saturated with injected powers of a few tens of milliwatts, which allows a low-power master oscillator and a low-power RF drive for a modulated system.

(3) Without injected power from the master oscillator, the amplifier emits only broadband spontaneous noise, which in the far field gives extinction ratios greater than 25 dB. As a result, single mode optical powers in excess of 1 W cw can be modulated with full digital on/off modulation.

(4) The spectral properties of the MFA-MOPA reflect those of the master oscillator, which is a narrow linewidth single spectral mode.

These attributes coupled with the rapid technical progress in MFA-MOPAs at 980 nm made the MFA-MOPA architecture a stronger candidate for achieving the goals of the NASA SCAR program. Therefore, during the first option year, the technical focus was redirected toward the realization of a MFA-MOPA architecture operating at 860 nm, i.e., with a GaAs quantum well active layer.

4.2. MFA-MOPAs at 860 nm

The design of the 860 nm MFA-MOPA, presented in Figure 4.2, is similar to the design of the 980 nm MFA-MOPA presented above. It consists of a distributed Bragg reflector (DBR) master

oscillator followed by a flared power amplifier. The epitaxial design consists of a GaAs quantum well active region surrounded by AlGaAs confining and cladding layers in a separate-confinement heterostructure. The gratings for the DBR master oscillator are second order with a period of approximately 257 nm. The single spatial mode output of the DBR laser is injected into the flared power amplifier where it diffracts and expands along the length of the power amplifier. The diffraction angle of the master oscillator signal within the flared amplifier is approximately 2.9°. An anti-reflection (AR) coating is deposited on the output aperture of the MFA-MOPA and has a reflectivity of approximately 0.1%. The MFA-MOPA is bonded p-side down on a patterned heatsink so the oscillator and amplifier can be individually addressed under cw operation.

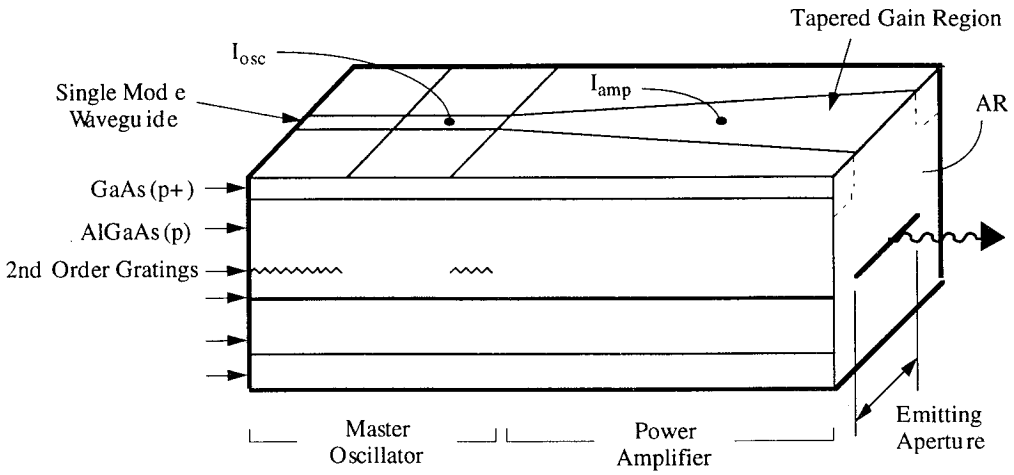

Figure 4.2. Schematic diagram of the 860 nm MFA-MOPA structure with an GaAs QW active region.

Although the architecture of an 860 nm MFA-MOPA is similar to that of the 980 nm MFA-MOPA previously demonstrated, there are several substantial technical issues unique to the 860 nm wavelength range. They are:

(1) The development of processes for grating formation and regrowth on high Al-containing materials;

(2) Investigation of the saturation characteristics of an 860 nm GaAs QW flared amplifier relative to those of a 980 nm InGaAs QW flared amplifier to obtain high saturation (for efficient energy extraction) and to minimize self-oscillation;

(3) Modifications to the chip and packaging to yield high speed modulation capability to greater than 0.5 GHz.

Two related research programs, NASA-SCAR and Rome Laboratories Advanced Development Model were directed to develop 860 nm MFA-MOPAs with somewhat different attributes;

NASA-SCAR focused on high-speed operation, while the emphasis of the Rome Laboratories program was upon high power operation and reliability. In the course of these programs, a common MFA-MOPA structure was developed that met the goals of both programs. The data presented in the following section describe the development of this common structure.

4.3 Initial MFA-MOPA Results

Initial 860 nm MFA-MOPA structures demonstrated results far superior to any other diffraction-limited chip architecture in this wavelength range, demonstrating output powers greater than 0.9 W cw and a far field pattern consisting of a single diffraction-limited lobe. A light-current (L-I) curve of a short wavelength MFA-MOPA is shown in figure 4.3. The L-I curve shows a slope efficiency of 0.6 W/A. The far field with the oscillator biased at drive currents of 0 and 80 mA are shown as an inset in figure 5.2. The far field with the oscillator on consists of a diffraction-limited lobe at a peak output power of 0.93 W cw. With the oscillator turned off, the peak power is reduced by greater than 15 dB. (The far field with the oscillator off is magnified 50 times in the inset.)

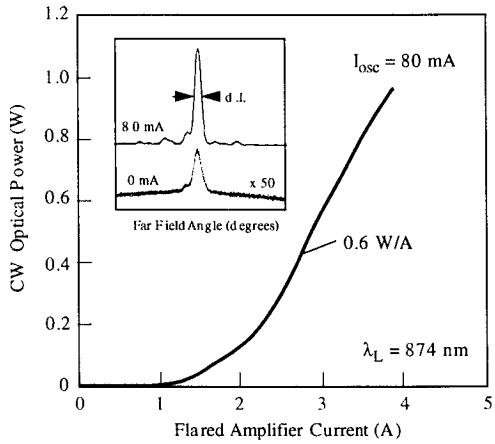

Figure 4.3. Schematic diagram of the GaAs MFA-MOPA.

Although the performance of a few of the best devices approached the NASA-SCAR goal specification of 1.0 W cw, the majority of devices demonstrated peak diffraction-limited powers of 0.5–0.6 W cw. The peak output power was limited in part by the relatively high turn-on current (>2 A) and in part by beam degradation at high bias currents. Therefore, further development of the 860 nm MFA-MOPA was directed toward improvements in high-power operation and reduction of the turn-on current.

4.4 Amplifier Length

One of the factors that affects the performance of MFA-MOPAs is feedback, which in turn is affected by the geometric magnification of the flared amplifier. In the MOPA, the DBR laser

supplies a small signal that is amplified in the flared amplifier. With a nonzero output reflectivity, there is a small (R~10^{-3}) return reflection from the output facet, which is amplified and further defocused as it propagates back to the master oscillator. A portion of the return signal is transmitted through the front grating into the master oscillator. In the desired mode of operation, the reverse traveling power from the amplifier transmitted through the front grating of the master oscillator is negligible compared to the reflected portion of the internally circulating power within the master oscillator. However, an undesirable mode of operation occurs when the returning power is comparable to or greater than the circulating signal.

The reflected power can be reduced by increasing the amplifier magnification, which is given by

$$M = \frac{2\theta L}{d}, \tag{4.1}$$

where d is the size of the single-mode waveguide (~3 μm), θ is the flare angle (~7°), and L is the length of the flare (2 mm in the first devices). To increase the magnification one can increase the length or flare angle or decrease the input waveguide size. In the 860 nm MFA-MOPA design, the waveguide could not be reduced below ~3 μm while maintaining low loss and the flare angle could not be increased beyond ~7° without incurring spherical aberration in the output beam; however, it was possible to increase the length of the amplifier, which in addition to increasing the magnification, would also reduce the operating current density and improve the reliability.

MFA-MOPAs were fabricated with amplifiers increased from 2.0 to 2.5 mm in length. The increased magnification had the desired effect of increasing the diffraction-limited operating power from 0.7–0.9 W cw to a typical value of 1.3 W cw power level. The power output from a MFA-MOPA with a 2.5 mm long amplifier is shown in Figure 4.4. The MFA-MOPA exhibits a turn-on current of 2.15 A and a slope efficiency of 0.64 W/A. The optical emission spectrum taken at an output power of 1.3 W is shown as an inset in the figure; it shows that the MFA-MOPA is operating in a single longitudinal mode with a side mode suppression ratio greater than 20 dB.

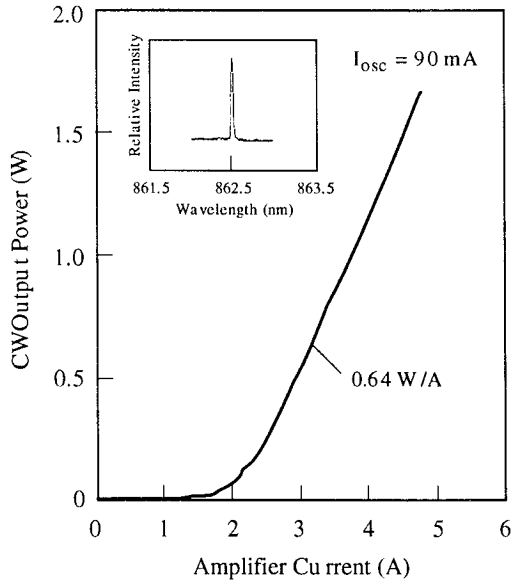

Figure 4.4. Total output power versus current for a MFA-MOPA with a 2.5 mm long amplifier. Shown as an inset is an optical emission spectrum taken at an output power of 1.31 W cw.

The far field of the MFA-MOPA is shown in Figure 4.5 at several power levels. The far field consists of a single diffraction-limited lobe to output powers in excess of 1.3 W with the vast majority of the power remaining in the main lobe. The FWHM of the main lobe is 0.17°, which is the diffraction limit for the 300 μm wide emitting aperture. Furthermore, the peak intensity of the main lobe increases approximately linearly with output power, indicating that the Strehl ratio is constant with increasing power. Separate measurements show that the far field does not steer as the output power is increased. Also shown is the far field pattern taken at an amplifier current of 4.25 A with the oscillator off. For clarity the zero reference for the oscillator-off data is offset from the other curves. With the oscillator off there is no detectable signal which, with the particular apparatus used, places the extinction ratio at a value greater than 25 dB.

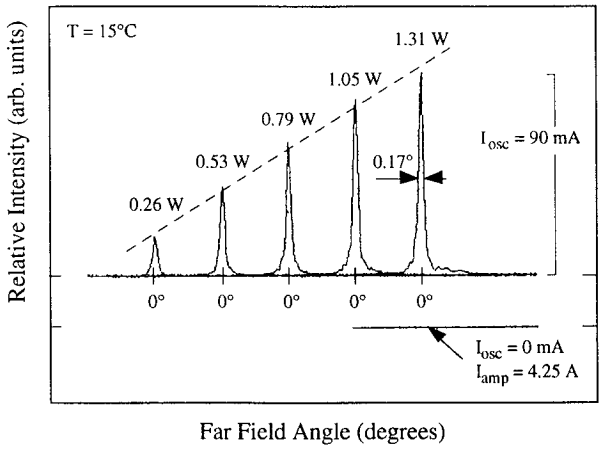

Figure 4.5. Far field patterns of the MFA-MOPA with a 2.5 mm long amplifier for various output powers.

4.5 Amplifier Gain Saturation

Among the differences between InGaAs quantum well MOPAs (at 980 nm) and GaAs quantum well MOPAs (860 nm) are the saturation characteristics of the different active layers. In general, InGaAs active layers have a larger differential gain, which leads to a lower saturation power. (The saturation power is the power level at which half of the injection current goes into stimulated emission.)

Figure 4.6 shows the output power for a 980 nm MFA-MOPA containing an InGaAs QW active region as a function of the master oscillator current keeping a constant current of 2.5 A to the flared amplifier. The figure shows that the gain of the flared amplifier is fully saturated at a master oscillator current of ~35 mA, which corresponds to an input power of 10-20 mW.

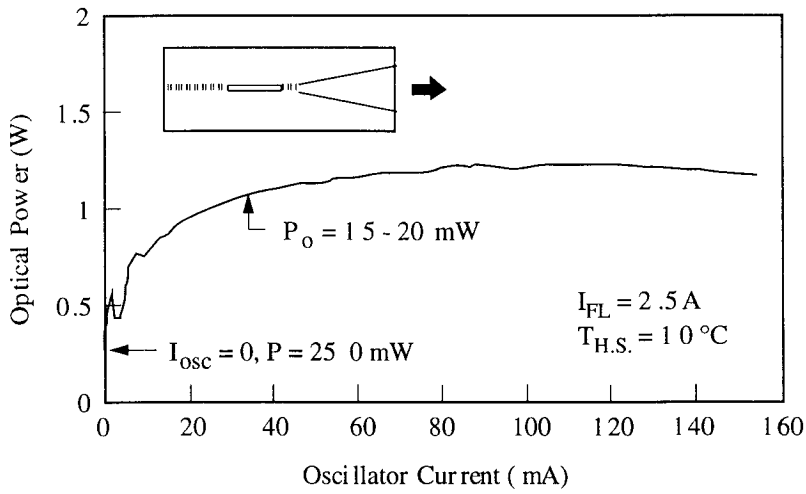

Figure 4.6. Saturation characteristics for a MFA-MOPA with a InGaAs QW active region operating at a wavelength of approximately 980 nm.

However, an appreciably higher power is needed to saturate the gain of 860 nm flared amplifier. Figure 4.7 shows the output power from a discrete flared amplifier from an 860 nm MFA-MOPA as a function of incident power from a Ti:sapphire laser. The saturation characteristics of the 860 nm amplifier are noticeably different. The 860 nm amplifier exhibits a slower saturation with injected power, requiring a coupled power of 50 mW (assuming a 50% coupling efficiency from the Ti:sapphire laser) for full saturation. The higher saturation powers for 860 nm amplifiers was verified by fabricating MFA-MOPAs and DBR lasers on the same 1 cm^2 wafer section. The saturation curves for the MFA-MOPAs are shown in Figure 4.8, which shows cw output power versus master oscillator current for various amplifier drive currents. A DBR threshold current of ~23 mA is apparent in these curves. The performance of the DBR lasers fabricated on the same wafer section was very uniform, allowing a calibration of integrated master oscillator current with output power. The result of this calibration is indicated on the upper x-axis scale. These data also show a slow gain saturation with a saturation power of approximately 50 mW, corroborating the experiments performed upon discrete amplifiers shown in figure 4.6.

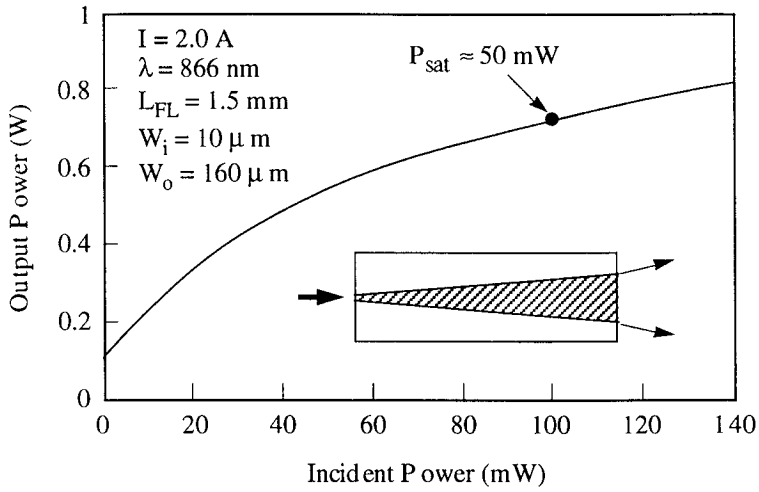

Figure 4.7. Saturation characteristics for a flared amplifier with a GaAs QW active region cleaved from a MFA-MOPA. The peak gain is at a wavelength of approximately 860 nm.

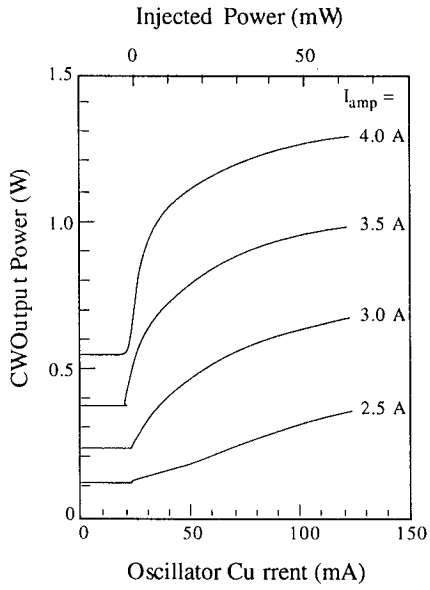

Figure 4.8. Saturation characteristics for a 860 nm MFA-MOPA with the master oscillator current also calibrated in output power.

As noted previously, turn-on currents in the 860 nm MFA-MOPAs were typically >2A, considerably higher than is found in InGaAs devices. The high turn-on currents combined with the higher required input power for full saturation indicated that the injected power from the DBR laser was low. Low injection power from the master oscillator only partially saturates the gain of the flared amplifier resulting in both higher turn-on currents and lower slope efficiencies. Master oscillators cleaved out from existing MFA-MOPAs confirmed that the DBR lasers were operating at low slope efficiencies and thus low output powers, resulting in higher turn-on currents and

higher amplifier gain to obtain a given output power. Unfortunately, the rate at which filamentation occurs (which degrades the far field and ultimately limits the beam quality of the device) is closely tied to the end-to-end amplifier gain. Thus, it was necessary to modify the epitaxial structure to increase the output power of the DBR master oscillators.

A new epitaxial structure was prepared with improved overlap between the quantum well active layer and reduced overlap with the grating layer (to lower the front grating reflectivity). Characterization of broad area lasers fabricated from this structure showed excellent performance, including an internal loss of 2 cm^{-1}, an internal efficiency of 87%, a transparent current density of 230 A/cm^2, and a characteristic temperature (T_o) greater than 180°K.

DBR lasers based on the new structure with front and rear grating lengths identical to those integrated into the MFA-MOPA were fabricated and tested separately. They achieved single mode operating powers greater than 100 mW cw, twice the power needed to saturate the gain of the flared amplifier. The new epitaxial structure was combined with a longer flared amplifier in a MFA-MOPA, and devices were processed and characterized.

MFA-MOPAs fabricated with the new epitaxial structure yielded a dramatically higher diffraction-limited operating power of 2.2 W cw. The light output as a function of the input current to the flared amplifier is presented in Figure 4.9. These data are taken at a heatsink temperature of 5°C with 150 mA of current to the master oscillator. Despite the larger amplifier chip area (associated with the longer amplifier), the turn-on current of the MFA-MOPA was actually reduced to 1.65 A (as compared to over 2 A previously). The maximum output power is 2.2 W cw at an input current of 5 A to the power amplifier. The slope efficiency of the power amplifier is 0.74 W/A (51%). Shown as an inset in the figure is an optical emission spectrum taken at an output power of 2.2 W. This spectrum indicates single longitudinal mode operation at a wavelength of approximately 854 nm with a side mode suppression ratio greater than 20 dB.

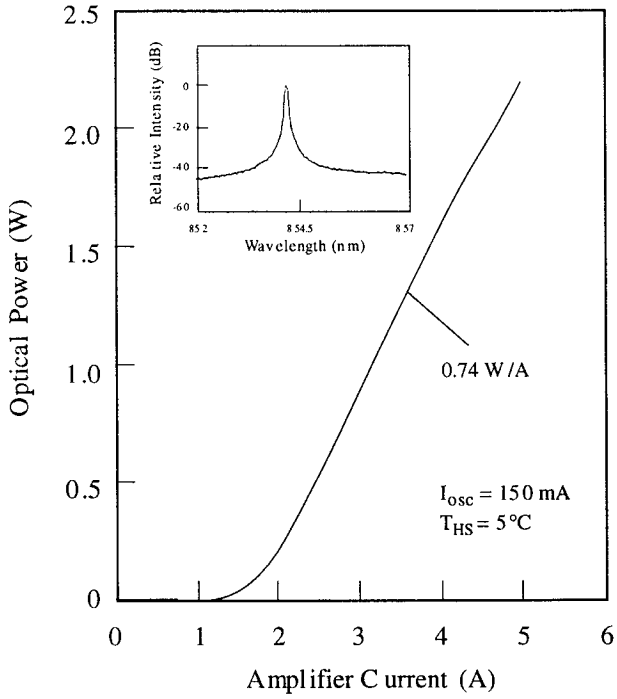

Figure 4.9. Light output-versus-input current to the flared amplifier with the master oscillator driven with 150 mA. The inset is an optical emission spectrum taken at an output power of 2.2.W cw.

The far field of the MFA-MOPA is presented in Figure 4.10. Far fields are characterized through a single multielement collimating lens with a focal length of 8 mm in order to remove the quadratic phase curvature introduced by diffraction within the amplifier. Far field patterns are shown with 150 mA driving the master oscillator for output powers between 0.92 and 2.2 W cw. At all operating powers, the far field maintains a predominantly single-lobed radiation pattern with a FWHM of 0.18°, the diffraction limit for the 280 μm wide emitting aperture of the flared amplifier. Furthermore, the peak intensity of the main lobe grows linearly with output power, implying that the Strehl ratio of the beam is constant as the output power is increased. Measurements of the root mean square variation of the phase front flatness, λ_{rms}, were found to be approximately $\lambda/16$ at the 1.2 W power level, indicating a Strehl ratio of approximately 0.85.

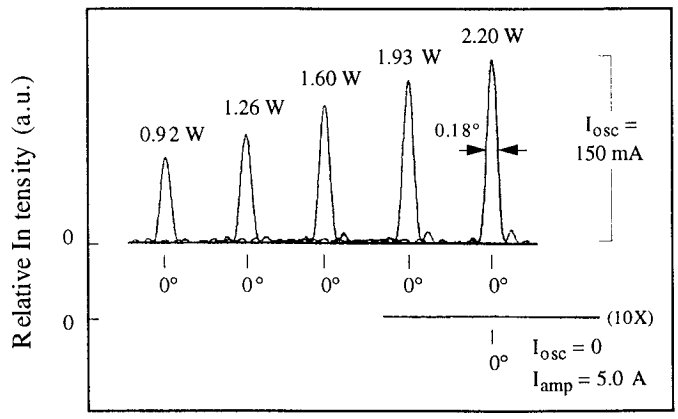

Figure 4.10. Far field patterns of the MFA-MOPA at output powers between 0.92 and 2.20 W cw. Also shown is the far field pattern, magnified by 10×, taken with the oscillator turned off and 5 A of current supplied to the amplifier.

A far field pattern (magnified 10-fold) is also shown in figure 4.10 that was taken with the oscillator turned off with 5 A of current to the power amplifier. Only amplified spontaneous emission is emitted from the MFA-MOPA when the oscillator is turned off. ASE is spectrally broadband and radiated at high angles and therefore does not overlap significantly with the diffraction-limited signal in the far field. Higher precision analysis of these data show that with the oscillator off and without the use of a spectral filter, the far field is extinguished by 26 dB with the oscillator off.

4.6 Beam Characterization

The output beam from all flared amplifiers possesses a built-in astigmatism due to the location of the virtual source point several hundred microns behind the emitting facet. The astigmatism is given approximately from geometric considerations by L/n_{eff}, where L is the length of the flared amplifier and n_{eff} is the effective index of the waveguide. In addition to the geometric component of the astigmatism, there are small corrections due to thermal and carrier effects.

Under cw operation, a slight variation in thermal lensing occurs within the amplifier as the result of the change in dissipated power with increasing drive current. The result is a slight change in the astigmatism of the output beam with output power. Figure 4.13 shows a schematic diagram of the depth of the virtual beam waist, D, as measured relative to the output facet. For 2.5 mm flared amplifiers, D is typically around 770 μm. The astigmatism can be easily removed with external optics (in fact, its presence allows for easy circularization of the beam). However, it is important for system applications that the variation in astigmatism under different operating conditions

remains well under a Rayleigh range to avoid changes in beam divergence or coupling efficiency in subsequent optics.

The change in virtual beam waist position ΔD normalized to the Rayleigh range Z_R is plotted as a function of output power in Figure 4.11. The Rayleigh range is given by $Z_R \equiv \pi w_0^2 / \lambda$, where $2w_0$ is the beam waist of the signal injected from the master oscillator. The output power was varied by adjusting the current to the amplifier while keeping the oscillator current constant. These measurements indicate that over the full operating range of the MFA-MOPA the total astigmatism change is less than $0.9Z_R$. Moreover, the astigmatism change saturates quickly to a constant value at an output power of 0.8 W. The quick saturation behavior of the lensing occurring within the amplifier shows that the output power can be increased by almost 3-fold from 0.8 W to 2.2 W cw without altering the astigmatism.

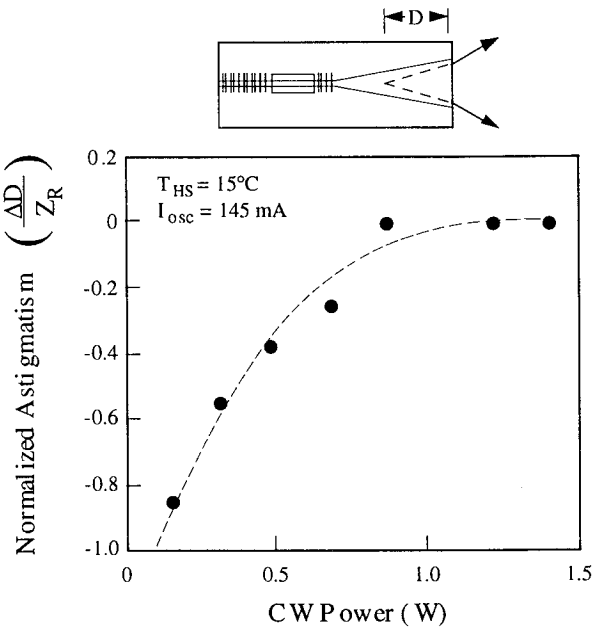

Figure 4.11. Normalized astigmatism of the output beam from the MFA-MOPA versus output power.

The change in astigmatism has also been characterized by varying the oscillator current while keeping the amplifier current constant. The results of these measurements are shown in figure 4.12. Under these conditions, the change in astigmatism also shows a saturation-like behavior where the total change in astigmatism changes by less than $0.6Z_R$ over the total operating range of the oscillator. The change in astigmatism approaches a constant value as the gain of the flared amplifier becomes more saturated due the increasing injected power from the master oscillator.

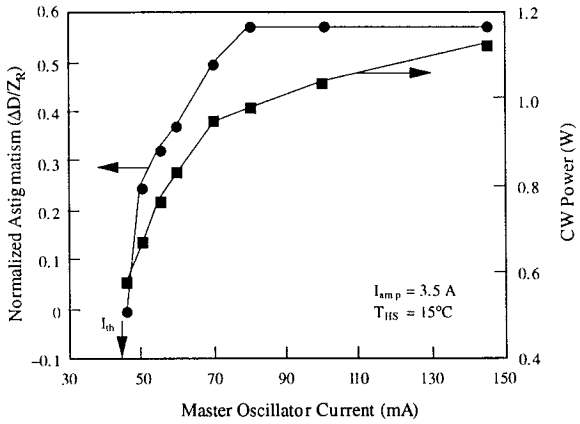

Figure 4.12. Normalized astigmatism of the output beam from a MFA-MOPA and the output power as a function of the current to the master oscillator.

Thus, the MFA-MOPA can be collimated and circularized with fixed optics to provide a diffraction-limited output over a wide range of drive currents to both the master oscillator and amplifier.

4.7 Modulation Capability

The MFA-MOPA design is ideally suited for high speed digital modulation of high coherent output power. The moderate injection power requirement for amplifier gain saturation, approximately 50 mW, enables large scale signal modulation of > 1 W output power with a very small change in input signal amplitude. The modulation goal of the NASA-SCAR program has been to demonstrate greater than 0.5 GHz modulation capability at the 0.5-1.0 W cw output power level in a diffraction-limited beam. As stated previously, the DBR master oscillator needs to produce only 50 mW of power to fully saturate the amplifier in the on state and the output power drops to zero when the master oscillator is turned off. However, in addition to power considerations, the modulation response of the master oscillator and parasitics of the laser and package must also be addressed.

For ease of bonding and high thermal conductivity, MFA-MOPAs were initially fabricated with large metal pads. Corresponding large pads were patterned on the submount to which the MFA-MOPAs were bonded. Although the large pads facilitate mounting and bonding, they also contribute a significant parasitic capacitance of 145 to 180 pF to the package, which can limit the high speed modulation capability of the MOPA.

High speed development centered on two tasks: development of a high-speed package and reduction of the parasitic capacitance of the submount and chip. The MFA-MOPA chip is mounted on a high thermal conductivity submount with separate contact pads for the amplifier and

the master oscillator. The master oscillator contact on the submount is kept narrow to minimize the capacitance. The submount/chip combination is mounted on a heatsink designed to accommodate a printed circuit board which is used to supply the high cw currents needed to power the amplifier. The tab of an SMA connector is brought into proximity to the master oscillator contact on the patterned submount.

The pads for the master oscillator on both the chip and submount were reduced in size to decrease the parasitic capacitance in the high speed configuration. Capacitances of several master oscillators from two different wafers have been measured at zero bias using an HP4277A LCZ capacitance meter. The measurements were carried out on the chip level and package level and are summarized in Figure 4.13. The figure shows average chip and package capacitances of 8 pF and 29 pF, respectively. With parasitics reduced to this level, the modulation performance could be evaluated at frequencies ranging up to several GHz.

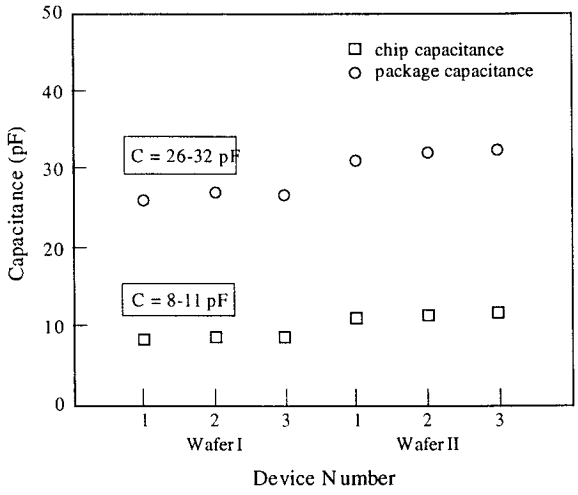

Figure 4.13. Capacitance of the master oscillator on the chip level and on the fully packaged level for several MFA-MOPAs from two separate wafers.

The small-signal frequency response of the MFA-MOPA was measured to determine bandwidth limitations due to electrical parasitics and intrinsic device response at a heatsink temperature of 15°C with the oscillator and amplifier driven at currents of 250 mA and 3.7 A, respectively. These test conditions correspond to an output power of approximately 1.2 W cw. The master oscillator was modulated using a low power RF signal supplied internally from an HP8719c network analyzer. A dc bias to the master oscillator was maintained with the use of a bias tee, while the modulated optical output was detected with a New Focus model 1434 detector. The photodiode output was routed back into the network analyzer with semi-flexible SMA cable for analysis. Since no attempt was made to match the impedance of the master oscillator to the measurement apparatus several attenuators were placed in the signal lines to minimize reflections.

Figure 4.14 shows the small signal amplitude response of an 860 nm MFA-MOPA packaged as shown in figure 4.13. The modulation response decreases by 3 dB at a frequency of approximately 1 GHz, twice the goal specification of 0.5 GHz. The frequency response appears to be limited by a pronounced dip which consistently appears at a frequency of approximately 1.5 GHz under all test conditions. The source of this dip has not been determined. The relaxation oscillation frequency under these drive conditions is 4.14 GHz. As expected from conventional laser theory, the relaxation oscillation frequency increased with master oscillator bias current linearly with the quantity $(I-I_{th})^{1/2}$. At lower dc biases to the master oscillator the frequency response was dominated by a 3 dB/octave roll-off. Even though a 6 dB/octave roll-off is expected for a simple single pole equivalent circuit, a 3 dB/octave roll-off behavior has been commonly observed under low bias conditions with high speed InGaAs QW lasers. The slower roll-off has been attributed to the existence of an effective capacitance in parallel with the parasitic capacitance. It has been suggested that the source of the effective capacitance is due to an extraneous carrier flow around the single mode waveguide.

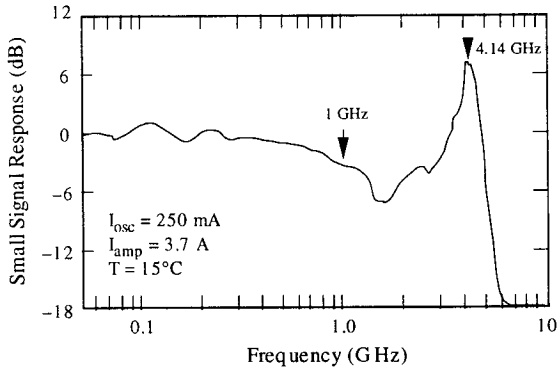

Figure 4.14. Small amplitude signal response for an 860 nm MFA-MOPA as a function of frequency.

Assuming that the dip at 1.5 GHz is due to either an artifact in the measurement system or due to a parasitic that can be eliminated, the frequency response of the 860 nm MFA-MOPA will be limited only by the relaxation oscillation frequency at ~4 GHz, almost an order of magnitude higher than the goal specification frequency.

5.0. SUMMARY

The NASA SCAR program began with the ambitious goal of developing an 860 nm diode laser source with a cw diffraction-limited output power some 5 times higher than anything demonstrated to date. In addition to the high power requirement, additional constraints were placed on the modulation capability, modulation rate, sidemode suppression ratio, and other spectral properties. At the close of the program, SDL demonstrated a device that exceeded every goal

specification by a considerable margin and delivered all contractual deliverables. The contract goals and SDL's performance are summarized in table 5.1 below.

Table 5.1. Goals and performance against goals.

Program Goal	**Program Achievement**
1 W cw	2.2 W cw
830–870 nm	860 nm
single longitudinal mode	single longitudinal mode, >20 dB sidemode suppression ratio
single spatial mode	single spatial mode, Strehl ratio~0.85
0.5 GHz modulation bandwidth	1.0 GHz small-signal modulation

The 860 nm MFA-MOPA operates to 2.2 W cw in a single diffraction limited output beam. The radiation pattern remains a stable, single-lobed high Strehl ratio beam with increasing operating current and does not steer. The astigmatism is fixed over large operating current ranges. The spectral output of the MFA-MOPA reflects that of the DBR master oscillator and is a single longitudinal mode. The far field extinguishes by 26 dB with the oscillator turned off making applications requiring high speed digital modulation possible.

A high speed package and bonding procedure was developed that enables modulation rates of 1 GHz or higher and, with a relaxation resonance as high as 4 GHz, offers the potential for further improvement. The combination of high diffraction-limited output power, high spatial and spectral mode quality, ease of modulation, high-speed operation, and 860 nm wavelength makes the MFA-MOPA an ideal candidate for high-data-rate satellite communications.

NASA REPORT DOCUMENTATION PAGE

1. Report No.	2. Government Accession No.	3. Recipient's Catalog No.

4. Title and Subtitle :	5. Report Date
Final Report Satellite Communications Applications Research	6. Performing Organization Code

7. Author (s)	8. Performing Organization Report No.
Robert J. Lang, Senior Research Section Manager, SDL, Inc.	10. Work Unit No..

9. Performing Organization Name and Address:	11. Contract or Grant No.:
SDL, Inc. 80 Rose Orchard Way San Jose, CA 95134	NASW - 4515

12. Sponsoring Agency Name and Address:	13. Type of Report and Period Covered
NASA Headquarters Headquarters Acquisition Division 300 7th St., SW Washington, DC 20546	Final Report 10/90 to 6/94
	14. Sponsoring Agency Code

15. Supplementary Notes

16. Abstract:: A 1 Watt diffraction-limited semiconductor laser diode has been demonstrated at 860 nm that provides single-longitudinel-mode operation, high modulation bandwidth, high beam quality and the unique ability to perform full modulation with a low-power electrical drive. The demonstrated device exceeds the goals of the contract and is a suitable source for optical space communications.

17. Key Words (Suggested by Author (s))	18. Distribution Statement
MOPA, Laser Diode, Diffraction-Limited, Single-Mode, High Speed	Unclassified

19. Security Classif. (of this Report)	20. Security Classif. (of this page)	21. No. of pages	22. Price
Unclassified	Unclassifed	35	